

Radiocarbon age offsets of foraminifera resulting from differential dissolution and fragmentation within the sedimentary bioturbated zone

Stephen Barker,¹ Wallace Broecker,² Elizabeth Clark,² and Irka Hajdas³

Received 3 August 2006; revised 17 November 2006; accepted 27 November 2006; published 1 May 2007.

[1] Shells of coexisting species of planktonic foraminifera from the Ontong Java Plateau reveal radiocarbon age offsets of up to 2200 years. Similar offsets are found between fragments and whole shells of single species. Steady state modelling of dissolution and bioturbation within the sedimentary mixed layer predicts age differences of up to several kiloyears due to the interplay between differential dissolution and fragmentation of foraminifer shells and bioturbation. The observation that fragile foraminiferal shells are systematically older than those of more robust species is more difficult to explain. Mechanisms of chemical erosion, interface dissolution, and sediment redistribution are all apparently unable to explain this phenomenon. A possible solution is presented in which a particular species may be represented by two distinct classes of shells which are more or less robust. In this case, differential dissolution and fragmentation causes an increase in the mean age as the fragile class contributes less to the remaining intact shells. This study highlights the vulnerability of low sedimentation rate cores to the effects of dissolution and bioturbation.

Citation: Barker, S., W. Broecker, E. Clark, and I. Hajdas (2007), Radiocarbon age offsets of foraminifera resulting from differential dissolution and fragmentation within the sedimentary bioturbated zone, *Paleoceanography*, 22, PA2205, doi:10.1029/2006PA001354.

1. Introduction

[2] Radiocarbon dates measured on foraminifer shells provide an important means of age model development for proxy records from sediment cores [e.g., *Stuiver et al.*, 1998]. They may also be utilised in reconstructing paleo-ventilation ages for the deep ocean [e.g., *Broecker et al.*, 2004; *Keigwin*, 2004] and paleoreservoir ages for the surface ocean [*Waelbroeck et al.*, 2001]. Yet several complications have been highlighted that may lead to significant uncertainties when attempting to interpret foraminiferal ^{14}C ages. These include the effects of bioturbation within the upper sediment column, faunal assemblage variations through time, secondary calcification, downslope transport and variations in atmospheric $\Delta^{14}\text{C}$ [*Peng and Broecker*, 1984; *Adkins and Boyle*, 1997; *Broecker et al.*, 1999b, 2006]. Here we describe the effects of another potentially complicating mechanism, that of differential dissolution and fragmentation of foraminiferal shells within the sedimentary bioturbated zone or mixed layer. We present a one-dimensional analytical model which we use to predict the potential effects of differential dissolution and fragmentation within the mixed layer. We then present new radiocarbon results from box core top sediments recovered from the Ontong Java Plateau, western equatorial Pacific. These results are discussed in light of the model predictions and several competing mechanistic explanations are discussed.

2. Processes Within the Bioturbated Zone

[3] The action of benthic organisms living within the upper few centimeters of sediment at the sea floor causes mixing of the sediments, effectively filtering or blurring records of potential oceanographic and climatic interest that may be captured by sedimentary components as they accumulate [*Peng et al.*, 1977; *Bard et al.*, 1987]. Of interest here is the effect on the ^{14}C age of foraminiferal shells and, in particular, the age offset between different species of foraminifera (benthic versus planktonic or planktonic versus planktonic). For example *Peng and Broecker* [1984] describe the hypothetical effect of bioturbation on benthic-planktonic (B-P) age differences for varying sedimentation rates. They show how mixing by bioturbation would cause a decrease in the magnitude of any change in the original signal and a shift of the signal back in time. The extent of the effect is inversely proportional to sedimentation rate. A more subtle complication stems from the interplay between bioturbation and changes in faunal assemblage through time. If a particular species of foraminifer (species x) became abundant in a given region, for example at the onset of the Holocene, then the action of bioturbation would cause the “down-mixing” of shells of species x into older sediments where none occurred before. If the down-mixed shells are then picked for radiocarbon dating, they will give a younger age than shells originally present at that horizon. Conversely, a reduction in species abundance may lead to anomalously old shells being “up-mixed” into younger sediments. In cases such as these the abundance change should be recognised and the anomalous age may be rejected. An example was described by *Manighetti et al.* [1995] for the appearance of *Globigerina bulloides* in the deglacial North Atlantic. Here, specimens of *G. bulloides* were found to be 2380 ^{14}C years younger than *Neoglobo-*

¹School of Earth, Ocean and Planetary Sciences, Cardiff University, Cardiff, UK.

²Lamont-Doherty Earth Observatory of Columbia University, Palisades, New York, USA.

³AMS 14C Laboratory, IPP ETH Hoenggerberg, Zurich, Switzerland.

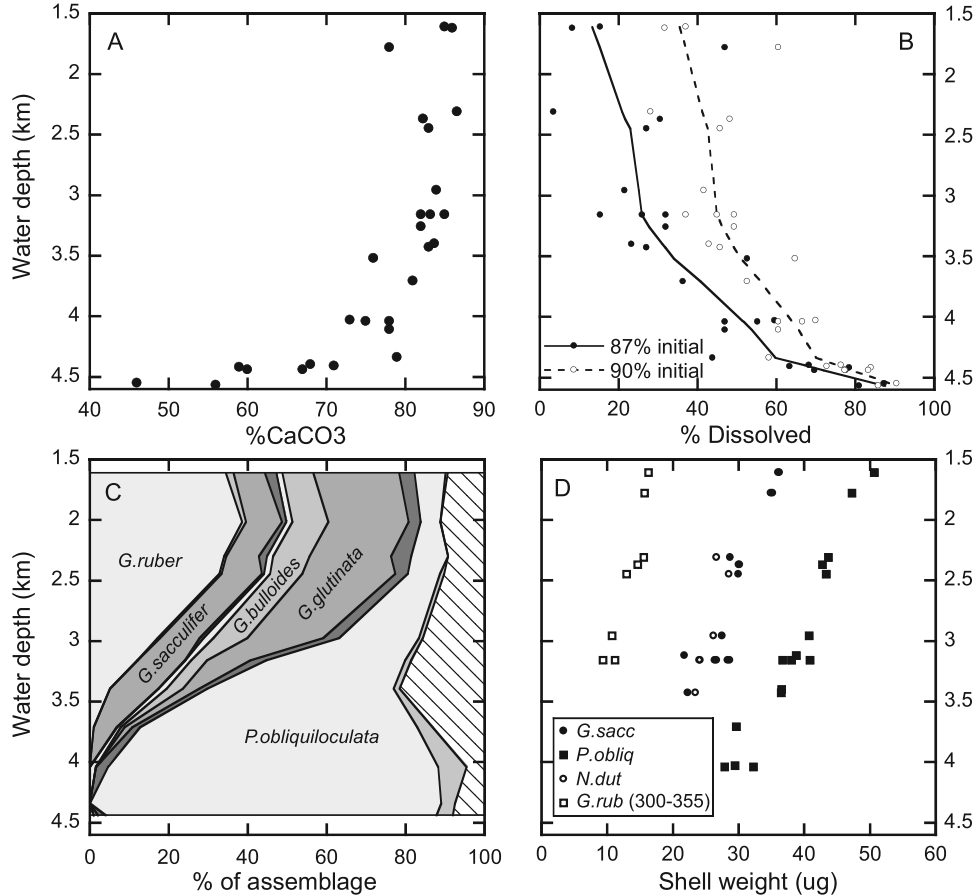


Figure 1. Results from the Ontong Java Plateau, western equatorial Pacific, show the effects of increased dissolution with water depth on the CaCO₃ content of surface sediments (a) and the corresponding extent of dissolution (b) assuming a constant initial CaCO₃ content of 87% or 90%. Also shown are the changes in planktonic foraminifer faunal assemblages (c) [Le and Thunell, 1996] and shell weights (d) [Broecker and Clark, 2001] from the same sites (shell weights are for the 355–425 μm fraction unless specified). Foraminiferal species in Figure 1c are arranged from left to right in order of decreasing susceptibility to dissolution according to Berger [1970] (*Globigerinoides ruber*, *Globigerina rubescens*, *Globigerinoides sacculifer*, *Globigerinoides tenellus*, *Globigerinoides conglobatus*, *G. bulloides*, *Globigerinita glutinata*, *Neogloboquadrina dutertrei*, *Pulleniatina obliquiloculata*, *Globorotalia tumida*, and others).

quadrina pachyderma (s) picked from the same interval. In this case the *G. bulloides* date was rejected since it was apparently down-mixed into older sediments.

[4] Dissolution of marine carbonates at the sea floor may occur under the influence of undersaturated bottom waters or due to the release of respiratory CO₂ (and consequent lowering of [CO₃²⁻]) within the upper few centimeters of sediment [Emerson and Bender, 1981]. The effects of dissolution on interspecies ¹⁴C ages would be unimportant but for the combination of two mechanisms: (1) Shells of different foraminiferal species tend to dissolve and fragment at different rates, and (2) bioturbation mixes together shells which have suffered varying degrees of dissolution and fragmentation. Fragmentation of planktonic foraminiferal shells at the sea floor is well known for its impact on faunal assemblages [e.g., Berger, 1970; Le and Thunell, 1996; Anderson and Archer, 2002] (Figure 1). Berger [1970] ranked 22 species of planktonic foraminifer according to

their susceptibility to dissolution and fragmentation. These differences may be due to the rates at which different species dissolve but must also relate to the varying thickness of their shells. For example a thin shelled, more fragile species may break up after losing 50% of its mass through dissolution whereas a thicker shelled, more robust species may survive until 70% of its shell has dissolved.

3. Simulating the Effects of Dissolution and Fragmentation Within the Mixed Layer

[5] The age distribution of any entity within the bioturbated or mixed layer will be approximately exponential [Andrée, 1987] (Figure 2). That is, assuming homogenous, infinitely fast mixing within a bioturbated zone of finite depth, shells of all ages between zero and infinity (or very old) will be present and the number of particles with any given age will decrease exponentially with increasing age

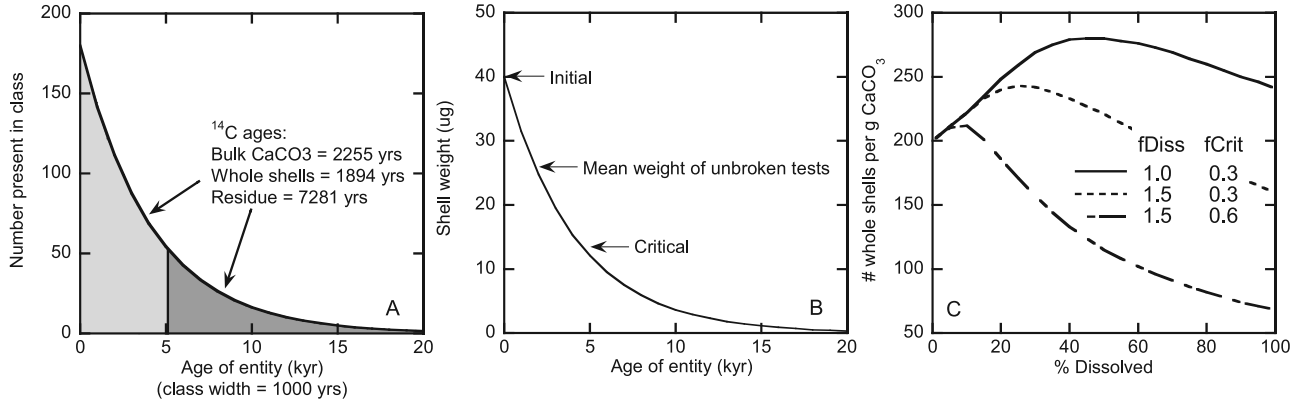


Figure 2. Modelled age distribution (a) and individual shell weight (b) of a hypothetical species of foraminifer within the sedimentary mixed layer. Shells break up below the critical weight which effectively decreases the measured ^{14}C age of picked, whole foraminifera. In this case, the initial CaCO_3 flux = 2 g/kyr, initial % CaCO_3 = 90%, dissolution of CaCO_3 within ML = 50%, and initial foram abundance = 200 shells per g CaCO_3 . (c) Increased dissolution within the ML causes changes in different species' abundance depending on their susceptibility to dissolution (f_{Diss} = dissolution rate factor, f_{Crit} = critical weight factor). Initially, the abundance per gram CaCO_3 increases for all species since individual shells dissolve by losing mass rather than breaking up. As the extent of dissolution increases, shells begin to break up and their abundance decreases. The relative abundance of robust (lower values of f_{Diss} and f_{Crit}) to fragile species increases with enhanced dissolution (see Appendix A for model description).

(assuming no change in initial abundance through time). If no dissolution occurred within the bioturbated layer, and assuming the initial weight of individual tests of a particular species were invariant through time, it would be straightforward to predict the mean age (and ^{14}C age) of that species within the mixed layer. However, the process of dissolution involves gradual thinning of foraminiferal shells and a corresponding decrease in weight for any shell as long as it remains in the mixed layer (where it may be prone to dissolution) [Broecker and Clark, 2001]. This will cause a skewing of the ^{14}C age toward the younger shells present, which are now heavier as well being more numerous than their older counterparts. This effect alone should not result in an offset between the ^{14}C ages of different species provided their rate of dissolution is proportional to their mass (see below). However, shells cannot continue to thin until they are infinitely light; at some point they will break up and fragment. At this point these “shells” will no longer count toward the mean ^{14}C age for that species since generally only whole shells are picked for dating (and many other chemical investigations). This means that the measured ^{14}C age will be biased toward the younger shells for any given species; the tail of older fragments will not be included (Figure 2). Furthermore, depending on the tendency for a particular species to break up, this biasing may be more or less significant, resulting in potential differences in the measured ^{14}C age of contemporaneous shells (Figure 3).

[6] In order to demonstrate the effects of differential dissolution and shell breakup of foraminifera within the mixed layer (ML) a simple analytical model was developed, based loosely on earlier models by Peng *et al.* [1977] and Broecker *et al.* [1984] but extended to treat species abundance, shell weights and shell fragmentation explicitly. The model assumes that dissolution occurs homogeneously

within the ML, which is defined as a zone of infinitely fast mixing. The rate of carbonate dissolution is defined as a proportion of the CaCO_3 raining to the sea floor. The rate of dissolution of foraminiferal shells is made proportional to the bulk CaCO_3 dissolution rate, depending on individual test mass with respect to the total mass of carbonate within the ML. A scaling factor (dissolution rate factor, f_{Diss}) is used to simulate enhanced (or the converse) dissolution with respect to bulk CaCO_3 . Breakup of shells occurs below a critical weight which is defined as a fraction of their initial weight (critical weight factor, f_{Crit}). Model equations are given in Appendix A.

[7] As the extent of dissolution within the ML increases the model predicts changes in the assemblage of foraminifer shells, depending on their particular susceptibility to dissolution (Figure 2). Initially, the abundance of whole shells per gram CaCO_3 increases for all species. This is because individual shells dissolve by losing mass but remain as entire entities within the ML while the absolute amount of CaCO_3 decreases (the proportion of noncarbonate material increases). As the extent of dissolution increases, the proportion of shells with a mass below f_{Crit} (for a given species) increases and so the abundance of whole shells decreases. The effect is exaggerated for shells dissolving at an enhanced rate relative to bulk CaCO_3 (increased f_{Diss}) and/or a higher critical weight threshold (increased f_{Crit}). The effect of these changes on predicted ^{14}C ages is shown in Figure 3. The bulk ^{14}C age of CaCO_3 within the ML decreases with increasing dissolution. This is characteristic of simulations employing homogeneous dissolution [Broecker *et al.*, 1984; Oxburgh, 1998] (see section 5). As discussed previously, the fragmentation of foraminiferal shells results in a biasing toward younger ages of the ^{14}C date attained from picking whole shells. The effect can be

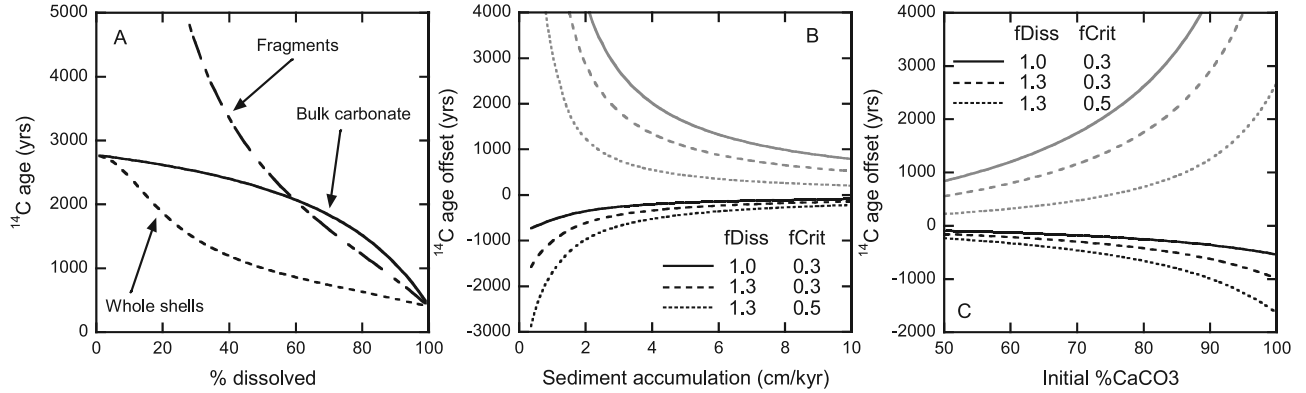


Figure 3. Simulated effects of differential dissolution and breakup of foraminiferal shells within the mixed layer in the case of homogeneous dissolution. (a) The mean ^{14}C age of bulk CaCO_3 within the ML decreases with increasing dissolution. Whole shells give younger ages than bulk CaCO_3 , with the largest offset occurring with $\sim 50\%$ dissolution while the offset between shell fragments and whole shells decreases with increasing dissolution. In this case, the delivery flux of CaCO_3 (set at 90% of bulk) is 2 g/kyr. Shells are dissolving at 1.5 times the rate of bulk CaCO_3 with a critical weight of 0.6 times the initial weight. Fragments are allowed to decrease to 50% of their weight on breakup before being ignored. (b) ^{14}C age offsets with bulk CaCO_3 for varying bulk sediment accumulation rates (obtained by varying the input flux of CaCO_3). Black curves are for whole shells, gray curves are for fragments. Initial sediment is 95% CaCO_3 , and dissolution is 50%. fDiss = dissolution rate factor and fCrit = critical weight factor. Fragments are included down to 50% of weight on breakup. (c) ^{14}C age offsets for varying initial sediment composition and initial CaCO_3 flux = 2 g/kyr; other parameters as for Figure 3b (see Appendix A for model description).

significant (>1000 years) for relatively low rates of sediment accumulation (≤ 3 cm/kyr) and is amplified for sediments with an initially high CaCO_3 content. The effect becomes less important as accumulation rates increase (>8 cm/kyr) and can also be reversed if fDiss < 1 . The largest ^{14}C age offset between bulk CaCO_3 and whole shells occurs when dissolution reaches about 50%. The calculated ^{14}C age of the fragmented shell material will be considerably older (up to 10 kyr) than the mean bulk CaCO_3 (Figure 2). To simulate an age for fragments that could reasonably be picked from a sample and dated, a further critical weight factor for fragments was included. This was typically set to 50% of their weight on fragmentation. Fragments are predicted to be several kiloyears older than their whole shell counterparts, with increased offsets for low rates of sediment accumulation (Figure 3). Additionally, fragments of more robust species should be older than the fragments of more fragile species.

[8] To give some impression of how values for fDiss and fCrit might apply to real sediments it is instructive to consider Figure 1, which shows results from the Ontong Java Plateau, western equatorial Pacific. Depending on the initial (before dissolution) CaCO_3 content of these sediments, somewhere between 35–55% has been dissolved by about 3.5 km water depth. In the same sediments the shell weights for various species of foraminifer have decreased by something like 30–40%. This will be a minimum since we do not actually know the original weight of these tests (they are already dissolving at the shallowest site). Furthermore, the mean weight of shells picked from these samples is, by definition, the mean weight of unbroken shells which

will be greater than the mean of the whole population if fragmented shells would be included. For example, using the model without fragmentation and fDiss = 1, the mean weight of shells in a mixed layer with 50% CaCO_3 dissolution will be half their initial weight. With the same extent of dissolution but a value of fCrit = 0.3, the average weight of unbroken shells is now 65% of their initial weight since those shells below fCrit are not counted (Figure 2b). Increasing fCrit to 0.5 causes the mean weight to increase to 75% initial. These results are in line with the sedimentary data shown in Figure 1 which suggests our chosen values of fDiss and fCrit are fairly realistic. It is interesting to note that the shell weight data shown in Figure 1 seem actually to require a value of fDiss not significantly less than 1. This suggests that fine fraction calcite may not dissolve significantly faster than foraminiferal calcite even though intuition suggests it might. Of course a range in both fDiss and fCrit must exist; the model sensitivity to such variations is illustrated in Figures 2 and 3 and gives some impression as to the range we may expect to find in nature.

4. South China Sea Sediments

[9] Broecker *et al.* [1988a] dated shells of *P. obliquiloculata* (a robust species) and *G. sacculifer* (fragile) from core V35-5 (7.2°N, 112.1°E, 1953 m) in the South China Sea. Their results revealed a systematic age offset between the two species with an average of about 900 years, with the more robust species giving older ages (Figure 4). This observation would be in line with the steady state, homogeneous dissolution model described here. On the other hand, results from nearby core V35-6 (7.2°N, 112.2°E,

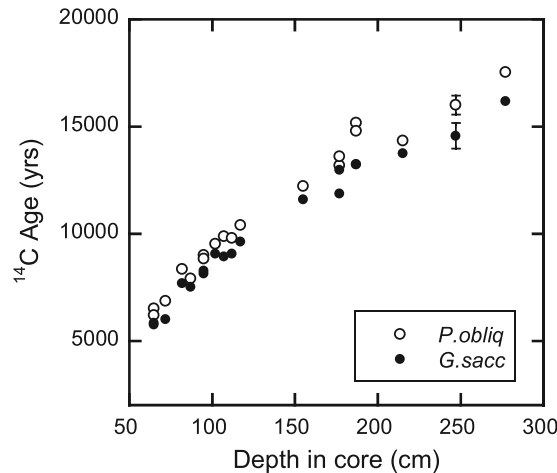


Figure 4. ^{14}C results for a robust (*P. obliquiloculata*) and fragile (*G. sacculifer*) species of foraminifer from a core from the South China Sea [Broecker et al., 1988a]. *P. obliquiloculata* give ages that are consistently older than *G. sacculifer* by an average of about 900 years. A core from a similar location revealed an average offset closer to 200 years.

2030 m) gave an average offset of more like 200 years. It seems unlikely that mixed layer conditions for sediments in such close proximity could be so different. For example, since values of fDiss and fCrit must be the same in both cases a difference of 700 years for a single species would require a shift of around 25–35% in the extent of dissolution. Given the similar water depths and overlying productivity conditions, we feel this is quite unlikely. Broecker et al. [2006] suggest instead that reworked shells of *P. obliquiloculata* may have been transported downslope, resulting in addition of older shells to the sample with presumably a higher proportion being added to V35-5. Their argument is that more robust shells

will survive reworking better than fragile ones; in this sense it provides a dynamic analogy to the mechanism described here. It may be suggested that part of the age offset may be due to the fact that *P. obliquiloculata* lives deeper in the water column than *G. sacculifer*. However, evidence from a very high sedimentation rate core from the western equatorial Pacific suggests that there is no systematic age offset between these two species [Broecker et al., 2004].

5. Results From the Ontong Java Plateau

[10] To further test the mechanism of differential dissolution and shell breakup on foraminiferal ^{14}C ages, we dated a number of whole shells and fragments for different species of planktonic foraminifer in box core top samples from multiple water depths on the Ontong Java Plateau (OJP), western equatorial Pacific (Table 1). From the results shown in Figure 1 we know that increased dissolution in deeper sites on the OJP results in decreased %CaCO₃, decreased foraminiferal shell weights [Broecker and Clark, 2001] and the dominance of robust species within foraminiferal assemblages [Le and Thunell, 1996]. We would therefore expect that fragments would be older than whole shells and robust species older than fragile ones. We may also expect individual species' ages to decrease with increasing water depth and dissolution. Our results are both surprising and confusing (Table 1 and Figure 5). ^{14}C ages for fragmented shells of *P. obliquiloculata* and *G. tumida* are considerably older (up to 2300 years) than for whole shells of the same species, in line with model predictions. However, the ages of individual species and of bulk CaCO₃ increase with water depth and increased dissolution. Furthermore, fragile species are consistently older than robust species (by up to 2200 years). Several possible explanations may be put forward to explain these observations.

[11] The fact that bulk CaCO₃ ^{14}C ages increase with water depth in the equatorial Pacific has been the subject of considerable enquiry [e.g., Keir, 1984; Broecker et al.,

Table 1. ^{14}C Results for the Ontong Java Plateau Core Tops Measured by AMS at ETH, Zurich^a

Core Number	Latitude°N	Longitude°E	Water Depth, km	Material	Wt, mg	14C Age, years	Error, years
MW91-9 BC36	0.0	158	2.32	<i>G.sacculifer</i>	20.2	3680	75
				<i>G.ruber</i>	13.1	4495	60
				<i>G.aequilateralis</i>	25.7	3395	50
				<i>P.obliquiloculata</i>	32.1	3300	50
				<i>G.tumida</i>	31.9	2270	55
				<i>Pobliq.</i> fragments	21.2	4345	70
				<i>G.sacculifer</i>	24.5	4560	55
				<i>G.aequilateralis</i>	24.3	3560	55
				<i>Pobliq.</i> (leach)	29.9	3240	55
				<i>Pobliq.</i> (residual)		3295	55
				<i>G.tumida</i> (leach)	44.6	2395	50
				<i>G.tumida</i> (residual)		2350	50
				<i>Pobliq.</i> fragments	24.7	4150	60
				<i>Pobliq.</i> (leach)	17.8	4040	55
				<i>G.tumida</i>	31.5	3270	50
MW91-9 BC56	0.0	162	4.04	<i>Pobliq.</i> (residual)	23.9	4180	55
MW91-9 BC74	0.0	163	4.44	<i>Pobliq.</i> fragments	26.9	3375	50
				<i>Pobliq.</i> fragments	19.7	5295	75
				<i>G.tumida</i> fragments	24.2	5750	55
				mixed fragments (<i>obl</i> + <i>tum</i>)	17.7	5425	60

^aAll samples represent the 0–3 cm interval. Ages are for whole shells unless otherwise indicated. The sample weights for the two leaching experiments are the combined weight of the leach and residual analyses.

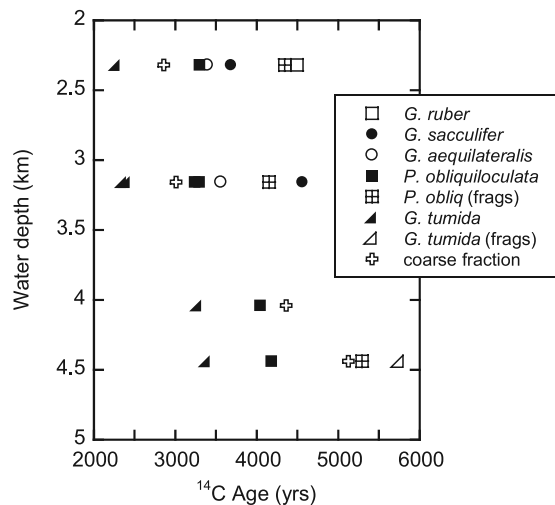


Figure 5. ¹⁴C results from Ontong Java Plateau core top samples. Fragments are up to >2300 years older than their whole shell counterparts. Bulk ¹⁴C ages increase with water depth and increasing dissolution, as do individual species ages. Robust species give younger ages than fragile species. Whole shells of *G. ruber* and *G. sacculifer* are essentially absent at deeper depths.

1991; *Oxburgh*, 1998]. For example, *Keir* [1984] suggested that the old ¹⁴C ages of deeper sediments in the Pacific Ocean may be explained by a recent (last few kiloyears) increase in dissolution intensity in the deep Pacific. The rate of CaCO₃ dissolution may increase to the point where it exceeds the rate of supply of CaCO₃ from the water column. At this point, chemical erosion will occur, bringing older sediments into the mixed layer and increasing the mean ¹⁴C age of core top samples. The effect would be greater in deeper waters where dissolution is more intense. This mechanism could explain the observation of increasing ¹⁴C ages with increasing water depth, but to explain the ¹⁴C age offset between individual species we would expect to find changes in the faunal assemblage below the core top. For example, to explain the particularly old age of *G. ruber* from core MW91-9 BC36 (Table 1) by the in-mixing of shells from lower down in the sediment column would require that *G. ruber* was relatively more abundant in deeper sediments. This could be either because the life assemblage had changed throughout the Holocene, or, as postulated by *Keir* [1984], because prior to a few thousand years ago dissolution was less intense, which would potentially mean that *G. ruber* was less prone to breakup. To investigate this idea we made faunal assemblage counts on down-core samples from MW91-9 BC36 (Figure 6). Apart from a slight increase in *G. sacculifer*, the fragile species show no increase in abundance with depth in core. Given an estimate of the accumulation rate of this core of around 2–3 cm/kyr [Broecker et al., 1999a] this record covers most of the Holocene. These findings suggest that chemical erosion cannot explain the large ¹⁴C age offsets observed between species.

[12] Another mechanism put forward to explain the old ¹⁴C ages of deep sediment core tops in the west equatorial Pacific is that of interface dissolution [Broecker et al., 1991; *Oxburgh*, 1998]. Interface dissolution describes the preferential dissolution of CaCO₃ before it is mixed into the bioturbated layer. The result of this process will be to effectively decrease the flux of CaCO₃ entering the sediments, thereby increasing the residence time of particles within the mixed layer. Increasing the extent of dissolution in this manner will therefore cause an increase in the mean ¹⁴C age of bulk CaCO₃ within the ML, as demonstrated by *Oxburgh* [1998]. While this mechanism can explain the older ¹⁴C ages of deeper samples it again seems to fail to explain the large offsets observed between species. This is because an age offset between any two entities must be due to a difference in the residence time of those entities within the ML. Whereas differential dissolution within the ML (as described earlier) can alter the residence times of various entities to different degrees, simply reducing the abundance of a particular species entering the ML (as implied by interface dissolution) cannot; the residence time of all entities will be controlled by the residence time of bulk CaCO₃.

[13] A possible explanation for the older ages of fragile species with respect to more robust shells, is that each species may have a range in its susceptibility to dissolution. Such differences could be a function of variations in initial shell calcification; it has been shown that single species of foraminifer can display significant differences in shell weight/thickness as a function of ambient conditions during growth [Barker and Elderfield, 2002]. It is easy to envisage that such variations in shell morphology might lead to differences in robustness. It is also plausible that multiple populations of a single species, distinct in their initial robustness, might occur effectively contemporaneously, possibly as a result of seasonal changes in growth conditions. In the simplest case a particular species may comprise two classes of shells, one more robust than the other. As dissolution proceeds, the mean ¹⁴C age of intact shells will tend toward that of the more robust population, which itself has a longer residence time in the ML; that is,

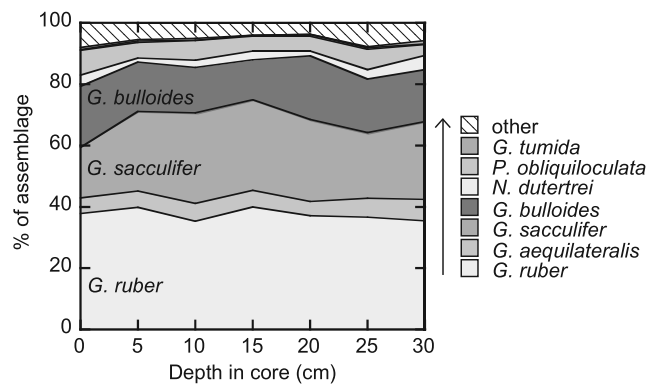


Figure 6. Faunal counts from MW91-9 BC36 show no particular down-core trend, suggesting that the old ¹⁴C ages of fragile species in the core top relative to more robust species are not the result of in-mixing of older shells.

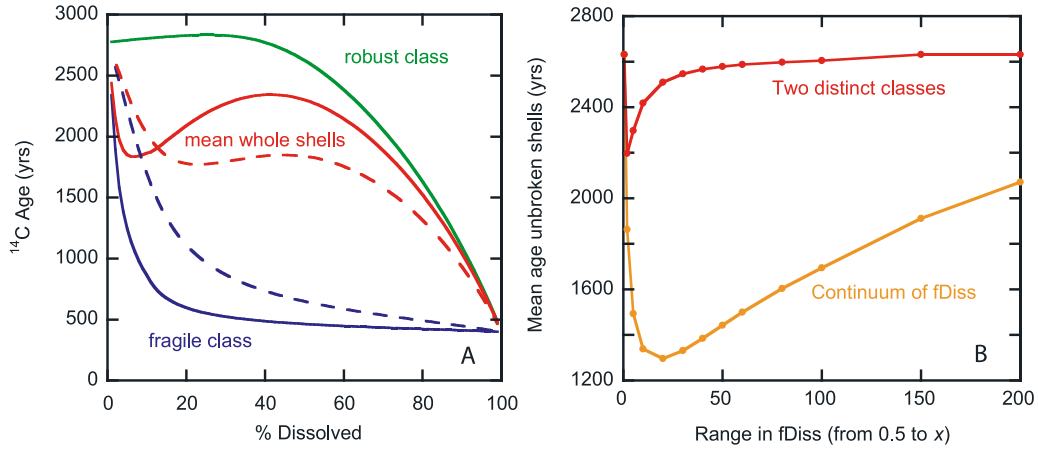


Figure 7. (a) Simulated ^{14}C ages for whole shells of two hypothetical foraminiferal species, each with two distinct classes of more or less robust shells. In both cases, the robust class (green curve) represents 20% of the initial composition ($f\text{Diss} = 0.5$, $f\text{Crit} = 0.3$). The blue curves represent the fragile class of a fragile species (solid line, $f\text{Diss} = 20$, $f\text{Crit} = 0.5$) and more robust species (dashed line, $f\text{Diss} = 5$, $f\text{Crit} = 0.5$). Red curves represent the combined ^{14}C age of whole shells from both classes for the fragile (solid line) and robust (dashed line) species. The fragile species gives generally older ages than the robust species. (b) Mean ^{14}C age of unbroken shells of a hypothetical species of foraminifer with a range in $f\text{Diss}$ for 50% CaCO_3 dissolution within the mixed layer (all shells have common initial weight, $f\text{Crit}$, and abundance). The red curve denotes a case with two distinct shell classes, whereas the orange curve represents a continuum of $f\text{Diss}$. In general, higher values for the maximum value of $f\text{Diss}$ lead to the mean age tending toward that of the more robust shells in the assemblage; that is, increasing the mean effective fragility causes an increase in age. The range of $f\text{Diss}$ required by the continuum case is unrealistically large.

the mean age of whole shells will get older. This can be demonstrated using the model described above and combining two hypothetical species to represent two classes within a single species (Figure 7). In this case combining two classes of shells with very different dissolution rates ($f\text{Diss} = 20$ and 0.5) results in an increase in the mean ^{14}C age of whole shells as dissolution increases from around 10 to 50% (solid red line in Figure 7a). If the combination is now changed to simulate a generally more robust species ($f\text{Diss} = 5$ and 0.5 for the two classes) the mean ^{14}C age of whole shells is systematically reduced for dissolution >10% (dashed red line in Figure 7a). Thus we attain older ages for a generally more fragile species. On the other hand, the same mechanism is less successful if a continuum of $f\text{Diss}$ is used to describe a range of “robustness” within a species. As an example, for 50% dissolution within the ML and a species with a continuum of $f\text{Diss}$ (where $f\text{Diss}$ varies linearly between 0.5 and some larger value, x), x must be >20 before the mean age of whole shells will increase for a further increase in x (i.e., for a further increase in fragility). To attain an increase of even 400 years in the mean age of unbroken shells would then require a range of $f\text{Diss}$ from 0.5 to 100. We believe such a high value for $f\text{Diss}$ is highly unlikely and therefore suggest that this mechanism requires rather distinct classes of shells as opposed to a continuum range in dissolution rate.

[14] A final mention should be made of sediment reworking and lateral redistribution. Broecker et al. [1999a] demonstrated that the rates of sediment accumulation within about 1 degree of the equator on the OJP are roughly twice

those just outside this zone. Higgins et al. [1999] presented excess ^{230}Th measurements from the same region. They showed that the accumulation of ^{230}Th in equatorial sediments was in excess of that produced in the overlying water column and that accumulating in off-equator sediments. Two possible explanations were put forward to explain these observations, the first posited that increased surface ocean biological production of organic and inorganic material above the equatorial sites could entrain a greater flux of clay and ^{230}Th during its fall to the sea floor. The second possibility is that physical transport processes could laterally redistribute sediments, resulting in preferential accumulation in a narrow equatorial-centred belt [Higgins et al., 1999]. This process is known as sediment focussing. Although the precise mechanism responsible for sediment focussing in this region has not been identified [Higgins et al., 1999] such redistribution could explain the presence of older fragments in the core top samples from the OJP; reworked shells are more likely to have broken up than those in situ. However, as pointed out by Broecker et al. [2006], reworking is most likely to result in older ages of robust species of foraminifera since these are more likely to survive redistribution than more fragile shells. On the other hand (as pointed out by one of the reviewers of this paper), it may be considered that lateral redistribution might be expected to transport smaller, lighter entities further and thus we may expect fragments to be older for this reason. The same argument could be made for lighter foraminifer shells such as *G. ruber* and *G. sacculifer*. This does seem to be an appealing explanation for the older ^{14}C age of these

species but since these same species are at the limit of surviving fragmentation (Figure 1) we believe they are unlikely to survive significant redistribution.

6. Potential Contamination From Secondary Calcite

[15] It may be envisioned that the addition of secondary calcite to individual foraminifer tests could be responsible for part of the ^{14}C age offset observed between species on the OJP. If addition of secondary calcite occurred after the material had been collected and equilibrated with modern atmospheric CO_2 this would cause an increase in the ratio of $^{14}\text{C}/^{12}\text{C}$ for any given entity and would thus tend to lower the measured ^{14}C age. In all likelihood the process might be expected to affect lighter and thinner walled shells more than heavier ones since the relative contribution of secondary calcite would be greater. This is contradictory to the observation that heavier shells (e.g., *P. obliquiloculata* and *G. tumida*) give younger ages than lighter, thinner walled species (e.g., *G. ruber* and *G. sacculifer*). On the other hand if secondary calcification occurred at the sea floor, within the original pore waters, where dissolved inorganic carbon may be considered to lie on a mixing line between old Pacific bottom waters and even older carbon from deeper sediments, this could effectively cause ageing of individual entities. However, even in the extreme case where calcite containing no radiocarbon is added, if the same mass of carbonate was added to two shells, one twice the mass of the other, the amount required to produce an offset of 2000 years (as observed between certain fragile/robust pairs) would be about 80% of the original mass of the lighter shell. The more likely situation where dissolved inorganic carbon did contain radiocarbon or where the original weight difference between shells was smaller, even more additional calcite would be required. To test the possibility that secondary calcite has played a role we used dilute acid to leach away part of the calcite from the two robust species from core MW91-9 BC63 (Table 1) with the idea that different phases of calcite might dissolve sequentially. Our results show no statistical age difference between the leached and residual calcite for either species. While this does not preclude the possibility that secondary calcite is present, it makes the case less likely.

7. Discussion and Further Testing

[16] There have been relatively few other studies dedicated to systematically dating multiple species of planktonic foraminifera but considering the magnitude of the age offsets reported here for the western Pacific we feel that further work is warranted. Broecker *et al.* [1988b] reported an inconsistent age offset between *G. bulloides* and *G. inflata* from a core in the North Atlantic (V23-81, 54.3°N, 16.8°W, 2393 m). In this core *G. bulloides* is occasionally older than *G. inflata* (fragile older than robust). The original authors could not identify a reason for the offset but we note that it is possibly not a consequence of dissolution and breakup given the depth of this core. We also note that Skinner and Shackleton [2004] report paired dates for *G. bulloides* and *N. pachyderma* (s) from the North

Atlantic (core MD99-2334 K, 37.8°N, 10.2°W, 3146 m) which reveal no such offset even though they are equally dissimilar in robustness according to Berger's [1970] ranking and both cores have a similar sedimentation rate. A potentially valuable test for the mechanisms of differential dissolution and shell breakup described here would be a systematic core top study in the deep Atlantic Ocean, where the history of recent dissolution may be rather different from (and perhaps more straightforward than) that in the deep Pacific.

[17] This study highlights the vulnerability of low sedimentation rate ($\leq 3 \text{ cm/kyr}$) cores and those suffering significant dissolution ($> \sim 30\%$ of initial CaCO_3) to the effects of fragmentation and bioturbation. This is not only relevant for studies involving radiocarbon measurements but also for any analysis which aims to determine precise temporal relationships between signals from different species of foraminifera (e.g. planktonic versus benthic records) or between foraminifera and other sedimentary archives (e.g., bulk sediment properties). In cases where sedimentation rates are low and/or dissolution plays a significant role, a minimum of two species of different "robustness" should be dated to test for the effects described here. It is difficult to quantify precisely the sedimentary conditions where these effects will have most impact but significant degrees of fragmentation or shell weight loss should raise awareness, similar to abundance changes for reliable age model development. Best practice would see multiple species analysed even for conditions where these effects might not be predicted.

8. Conclusions

[18] Differential dissolution and fragmentation of foraminiferal shells within the sedimentary bioturbated zone or mixed layer can cause significant (several kiloyears) offsets in the measured ^{14}C age between different species and between the fragments and whole shells of individual species. Offsets are largest for lower rates of sediment accumulation ($\leq 3 \text{ cm/kyr}$) and for sediments with initially high CaCO_3 content. We have demonstrated that significant (up to 2200 years) offsets exist between ^{14}C ages of coexisting species of planktonic foraminifera within sediments accumulating on the Ontong Java Plateau. We have also reported ^{14}C age offsets between whole shells and fragments of the same species of up to 2300 years. While the steady state, homogeneous model described here is able to predict similar magnitudes of offsets between fragments and whole shells and between species, it is unable to predict the observation that fragile shells are older than more robust species' shells unless a range of susceptibility to dissolution is called upon. Mechanisms of chemical erosion, interface dissolution and lateral sediment transport are also unable to explain the older ages of fragile species. Regardless of the precise mechanism responsible, the fact that age differences between coexisting species of planktonic foraminifera as large as 2200 years are found in sediment accumulating at a rate of about 3 cm/kyr has implications for many paleoceanographic studies. In particular, caution must be taken in oceanic regions where sedimentation rates are generally low and bottom waters corrosive, such as the open Pacific Ocean. Even in sediments with higher rates of accumula-

tion, assuming the observed differences are inversely proportional to sedimentation rate, an age offset as high as 700 years could occur in a sediment accumulating at 10 cm/kyr. This emphasises the need to obtain cores with high sedimentation rates and suffering minimal dissolution.

Appendix A: Model Description

A1. Parameters

CaCO_3in	Flux of CaCO_3 into ML ($\text{g}/\text{cm}^2/\text{ka}$)
f_{sin}	Carbonate fraction of raining sediment
z	Thickness of mixed layer (centimeters)
fD	Fraction of raining carbonate dissolved in ML
Age_{surf}	Reservoir age of surface ocean (years)
$\text{Abund}_{\text{Xin}}$	Abundance of species X entering ML (number/ gCaCO_3)
Wt_{Xin}	Initial individual shell weight of species X (10^{-6}g)
f_{Diss}	Species specific dissolution rate factor
f_{Crit}	Species specific critical weight factor
$^{14}\text{C}_{\text{atm}}$	Atmospheric $^{14}\text{C}/\text{C}$ ratio (set = 1)
λ	^{14}C decay constant (= 1/8033) (using Libby half life)
Sed_{in}	Sediment flux into ML ($\text{g}/\text{cm}^2/\text{ka}$) = $\text{CaCO}_3\text{in}/f_{\text{sin}}$
D	Rate of CaCO_3 dissolution in ML ($\text{g}/\text{cm}^2/\text{ka}$) = $\text{CaCO}_3\text{in} \times fD$
CaCO_3out	Flux of CaCO_3 out of ML ($\text{g}/\text{cm}^2/\text{ka}$) = $\text{CaCO}_3\text{in} - D$
Sed_{out}	Sediment flux out of ML ($\text{g}/\text{cm}^2/\text{ka}$) = $\text{Sed}_{\text{in}} - D$
f_{SML}	Fraction of carbonate in ML = $\text{CaCO}_3\text{out}/\text{Sed}_{\text{out}}$
ρ	Density of ML sediment (g/cm^3) see equation (A1)
CaCO_3ML	Mass of CaCO_3 within ML (g) = $\rho \times z \times f_{\text{SML}}$
A	Sediment accumulation rate (cm/ka) = $\text{Sed}_{\text{out}}/\rho$
τ	Residence time of silt grains in ML (years) = $1000 \times z/A$
$^{14}\text{C}_{\text{surf}}$	$^{14}\text{C}/\text{C}$ ratio in surface ocean = $^{14}\text{C}_{\text{atm}} \times \exp(-\lambda \times \text{Age}_{\text{surf}})$
$^{14}\text{C}_{\text{in}}$	$^{14}\text{C}/\text{C}$ ratio of CaCO_3 into ML $\approx ^{14}\text{C}_{\text{surf}}$
Wt_{Xcrit}	Critical weight of foram shell at breakup (10^{-6}g) = $\text{Wt}_{\text{Xin}} \times f_{\text{Crit}}$
$^{14}\text{C}_{\text{ML}}$	$^{14}\text{C}/\text{C}$ ratio of carbonate within ML
$^{14}\text{C}_{\text{ageML}}$	^{14}C age of carbonate within ML (^{14}C years)
$\text{Abund}_{\text{XML}}$	Abundance of species X in ML (ignoring breakup) (number/ gCaCO_3)
$\text{Abund}_{\text{XML}}$	Abundance of unbroken tests of species X in ML (number/ gCaCO_3)
$\text{Abund}_{\text{XML},t}$	Abundance of species X with age t in ML (number/ gCaCO_3)
Wt_{XML}	Mean shell weight of unbroken tests of species X in ML (10^{-6}g)
$\text{Wt}_{\text{XML},t}$	Individual shell weight of species X with age t in ML (10^{-6}g)

$\#_{\text{XML}_t}$	Number of tests of species X with age t in ML
$\#_{\text{XML}}$	Number of unbroken tests of species X in ML
T_{Xcrit}	Age of species X at breakup within ML (kiloyears)
$^{14}\text{C}_{\text{Xin}}$	$^{14}\text{C}/\text{C}$ ratio of species X entering ML
$^{14}\text{C}_{\text{XML}}$	$^{14}\text{C}/\text{C}$ ratio of unbroken tests of species X within ML
$^{14}\text{C}_{\text{ageXML}}$	^{14}C age of unbroken tests of species X within ML (^{14}C years)
$^{14}\text{C}_{\text{ageFragXML}}$	^{14}C age of fragmented tests of species X within ML (^{14}C years)

[19] Note: The Libby half life of 5568 years is used here for consistency with conventional radiocarbon measurements; the difference between two conventional ^{14}C ages will be about 3% shorter than the absolute offset. This is simply demonstrated; for two samples, P and B, the conventional radiocarbon ages are defined as, ^{14}C age $(P) = -8033 \times \ln(A_P/A_{\text{standard}})$, ^{14}C age $(B) = -8033 \times \ln(A_B/A_{\text{standard}})$ where A is the activity of ^{14}C . Therefore the difference between two conventional radiocarbon ages; ^{14}C age $(B-P) = -8033 \times \ln(A_B/A_P)$. The absolute age difference, using a half life of 5730 years will be, $\Delta T = -8267 \times \ln(A_B/A_P)$. Therefore $\Delta^{14}\text{C}$ age $(B-P) = \Delta T \times 8033/8267$.

A2. Background

[20] Sediment density, ρ , defined by Oxburgh [1998] after Murray [1987]:

$$\rho = 1/(4.207 - 0.95 \times (3.395 \times f_{\text{SML}})) \quad (\text{A1})$$

[21] According to Broecker and Peng [1982] and Andrée [1987] the mean ^{14}C age of CaCO_3 in the ML is given by:

$$\text{Age} = 8033 \times \ln(1 + \tau/8033) \quad (\text{A2})$$

[22] Broecker et al. [1984] redefined this to account for dissolution:

$$\text{Age} = 8033 \times \ln(1 + (1 - fD) \times \tau/8033) \quad (\text{A3})$$

A3. One Box Model of the Mixed Layer

[23] Assuming a homogenous mixed layer (i.e., infinite mixing throughout) the rate of change of ^{14}C activity within the mixed layer can be expressed as

$$\partial^{14}\text{C}_{\text{ML}}/\partial t = (^{14}\text{C}_{\text{in}} \times \text{CaCO}_3\text{in} - ^{14}\text{C}_{\text{ML}} \times (\text{CaCO}_3\text{out} + D + \lambda \times 1000 \times \text{CaCO}_3\text{ML})) / (1000 \times \text{CaCO}_3\text{ML})$$

[24] At steady state:

$$^{14}\text{C}_{\text{ageML}} = 8033 \times \ln(1 + (1 - fD) \times \tau/8033) + \text{Age}_{\text{surf}} \quad (\text{A4})$$

[25] This is equivalent to equation (A3).

A4. Effect of Dissolution on Foraminiferal Tests Within the Mixed Layer

A4.1. Species Abundance Without Breakup

[26] At steady state (ignoring shell breakup) the number of shells of species X within the ML is constant:

$$\text{Abund}_{\text{XML}}' = \text{Abund}_{\text{Xin}} / (1 - fD) \quad (\text{A5})$$

[27] The number of shells with age t is given by:

$$\#_{\text{XML}t} = \text{Abund}_{\text{Xin}} \times \text{CaCO}_{3\text{in}} \times \exp(-1000t/\tau) \quad (\text{A6})$$

A4.2. Weight Loss

[28] Dissolution of foraminiferal tests is expressed as weight loss as a function of the total rate of CaCO_3 dissolution within the ML:

$$\begin{aligned} \partial \text{Wt}_{\text{XML}t} / \partial t &= -\text{Wt}_{\text{XML}t} \times fD \times D / \text{CaCO}_{3\text{ML}} \\ \text{Wt}_{\text{XML}t} &= \text{Wt}_{\text{Xin}} \times \exp(-t \times Df_X \times fD \times 1000 \\ &\quad / ((1 - fD) \times \tau)) \end{aligned} \quad (\text{A7})$$

where t is measured in kiloyears. $\text{Wt}_{\text{XML}t}$ refers to the weight of an individual shell at time t after entering the ML as opposed to the average weight.

A4.3. Shell Breakup

[29] Fragmentation of shells within the ML is represented by breakup below a critical weight:

$$\text{Wt}_{\text{Xcrit}} = f\text{Crit} \times \text{Wt}_{\text{Xin}}$$

[30] Although shell material is still present in the ML after breakup, it will generally not be picked for analysis and is therefore not included in our calculation of mean shell weight and ^{14}C age within the ML.

[31] The age at which breakup occurs depends on the rate of shell weight loss and the critical weight:

$$T_{\text{Xcrit}} = [\ln(1/f\text{Crit})] \times (1 - fD) \times \tau / (fD \times fD \times 1000) \quad (\text{A8})$$

where T_{Xcrit} is measured in kiloyears. The total number of unbroken shells of species X within the ML at any time is the integration of shells with ages between 0 and T_{crit} :

$$\begin{aligned} \#_{\text{XML}} &= \int_0^{T_{\text{Xcrit}}} \#_{\text{XML}t} dt \\ \#_{\text{XML}} &= \text{Abund}_{\text{Xin}} \times \text{CaCO}_{3\text{in}} \\ &\quad \times [(-\tau/1000) \times \exp(-1000 \times t/\tau)]_0^{T_{\text{Xcrit}}} \end{aligned} \quad (\text{A9})$$

A4.4. Species Abundance With Breakup

[32] Incorporating shell breakup into the model, the abundance of species X within the ML is given by

$$\begin{aligned} \text{Abund}_{\text{XML}} &= \text{Abund}_{\text{Xin}} \times \text{CaCO}_{3\text{in}} \times [(-\tau/1000) \\ &\quad \times \exp(-1000 \times t/\tau)]_0^{T_{\text{Xcrit}}} / \text{CaCO}_{3\text{ML}} \end{aligned} \quad (\text{A10})$$

A4.5. Mean Shell Weight

[33] The mean weight of unbroken tests of species X within the ML will be the integration of shell weights of all ages $\leq T_{\text{Xcrit}}$ within the ML divided by the number of unbroken shells:

$$\begin{aligned} \text{Wt}_{\text{XML}} &= \left(\int_0^{T_{\text{Xcrit}}} \text{Wt}_{\text{XML}t} \times \#_{\text{XML}t} dt \right) / \#_{\text{XML}} \\ \text{Wt}_{\text{XML}} &= \text{Wt}_{\text{Xin}} \times \text{Abund}_{\text{Xin}} \times \text{CaCO}_{3\text{in}} \\ &\quad \times [(1/a) \times \exp(at)]_0^{T_{\text{Xcrit}}} / \#_{\text{XML}} \end{aligned} \quad (\text{A11})$$

where $a = -1000(1 + (Df_X \times fD / (1 - fD))) / \tau$

A4.6. ^{14}C Age of Species X

[34] The ^{14}C age of unbroken tests of species X within the ML is given by

$$^{14}\text{C}_{\text{ageXML}} = (1/\lambda) \times \ln\left(^{14}\text{C}_{\text{atm}} / ^{14}\text{C}_{\text{XML}}\right) \quad (\text{A12})$$

where $^{14}\text{C}_{\text{XML}} = (\int_0^{T_{\text{Xcrit}}} \text{Wt}_{\text{XML}t} \times \#_{\text{XML}t} \times ^{14}\text{C}_{\text{XML}t}) / (\int_0^{T_{\text{Xcrit}}} \text{Wt}_{\text{XML}t} \times \#_{\text{XML}t})$

and $^{14}\text{C}_{\text{XML}} = ^{14}\text{C}_{\text{Xin}} \times e^{-1000\lambda t}$

$$\begin{aligned} ^{14}\text{C}_{\text{XML}} &= ^{14}\text{C}_{\text{Xin}} \times [(1/b) \times \exp(bt)]_0^{T_{\text{Xcrit}}} \\ &\quad / [(1/a) \times \exp(at)]_0^{T_{\text{Xcrit}}} \end{aligned}$$

where $a = -1000(1 + (Df_X \times fD / (1 - fD))) / \tau$ and $b = -1000(\lambda + (1/\tau) + (Df_X \times fD / \tau(1 - fD)))$

A4.7. ^{14}C Age of Fragmented Tests of Species X

[35] The ^{14}C age of fragmented tests of species X within the ML is then

$$^{14}\text{C}_{\text{ageFragXML}} = (1/\lambda) \times \ln\left(^{14}\text{C}_{\text{atm}} / ^{14}\text{C}_{\text{FragXML}}\right) \quad (\text{A13})$$

where $^{14}\text{C}_{\text{FragXML}} = ^{14}\text{C}_{\text{Xin}} \times [(1/b) \times \exp(bt)]_{T_{\text{Xcrit}}}^{\infty} / [(1/a) \times \exp(at)]_{T_{\text{Xcrit}}}^{\infty}$

[36] This age will represent fragments of all sizes. If the fragments to be dated are within a similar size fraction as used for whole shells (i.e., have a minimum size comparable to unbroken shells), the upper time limit should be reduced. Here we use an age when the fragments have dissolved to a factor x of the weight at which the shell fragmented (i.e., when $\text{Wt}_{\text{XML}t} = \text{Wt}_{\text{Xcrit}} \times x$):

$$\text{Wt}_{x\text{Xcrit}} = x \times f\text{Crit} \times \text{Wt}_{\text{Xin}}$$

$$^{14}\text{C}_{\text{ageFragxXML}} = (1/\lambda) \times \ln\left(^{14}\text{C}_{\text{surf}} / ^{14}\text{C}_{\text{FragxXML}}\right) \quad (\text{A14})$$

where $^{14}\text{C}_{\text{FragxXML}} = ^{14}\text{C}_{\text{Xin}} \times [(1/b) \times \exp(bt)]_{T_{\text{Xcrit}}}^{T_{x\text{Xcrit}}} / [(1/a) \times \exp(at)]_{T_{\text{Xcrit}}}^{T_{x\text{Xcrit}}}$

where $T_{x\text{Xcrit}} = [\ln(1/x \times f\text{Crit})] \times (1 - fD) \times \tau / f\text{Diss} \times fD \times 1000$

[37] **Acknowledgments.** We would like to thank Dan McCorkle for generously supplying the samples used in this study and Heather Griffith for performing the faunal counts. We thank Jerry Dickens (Editor), Luke

Skinner, and an anonymous reviewer for their thoughtful and detailed comments. This work was supported by NSF grant OCE-0435703.

References

- Adkins, J. F., and E. A. Boyle (1997), Changing atmospheric $\Delta^{14}\text{C}$ and the record of deep water paleoventilation ages, *Paleoceanography*, **12**, 337–344.
- Anderson, D. M., and D. Archer (2002), Glacial-interglacial stability of ocean pH inferred from foraminifer dissolution rates, *Nature*, **416**, 70–73.
- Andrée, M. (1987), The impact of bioturbation on AMS ^{14}C dates on handpicked foraminifera: A statistical model, *Radiocarbon*, **29**, 169–175.
- Bard, E., M. Arnold, J. Duprat, J. Moyes, and J. C. Duplessy (1987), Reconstruction of the last deglaciation: Deconvolved records of $\delta^{18}\text{O}$ profiles, micropaleontological variations and accelerator mass spectrometric ^{14}C dating, *Clim. Dyn.*, **1**, 101–112.
- Barker, S., and H. Elderfield (2002), Foraminiferal calcification response to glacial-interglacial changes in atmospheric CO_2 , *Science*, **297**, 833–836.
- Berger, W. H. (1970), Planktonic foraminifera: Selective solution and the lysocline, *Mar. Geol.*, **8**, 111–138.
- Broecker, W. S., and E. Clark (2001), An evaluation of Lohmann's foraminifera weight dissolution index, *Paleoceanography*, **16**, 531–534.
- Broecker, W. S., and T.-H. Peng, (1982), *Tracers in the Sea*, Lamont-Doherty Earth Observatory, Palisades, N. Y.
- Broecker, W. S., A. Mix, M. Andrée, and H. Oeschger (1984), Radiocarbon measurements on coexisting benthic and planktic foraminifera shells: Potential for reconstructing ocean ventilation times over the past 20000 years, *Nucl. Instrum. Methods Phys. Res. Sect. B*, **5**, 331–339.
- Broecker, W. S., et al. (1988a), Accelerator mass-spectrometry radiocarbon measurements on marine carbonate samples from deep-sea cores and sediment traps, *Radiocarbon*, **30**, 261–295.
- Broecker, W. S., M. Andree, W. Wolfli, H. Oeschger, G. Bonan, J. P. Kennett, and D. Peteet (1988b), The chronology of the last deglaciation: Implications to the cause of the Younger Dryas event, *Paleoceanography*, **3**, 1–19.
- Broecker, W. S., M. Klas, and E. Clark (1991), The influence of CaCO_3 dissolution on the core top radiocarbon ages for deep-sea sediments, *Paleoceanography*, **6**, 593–608.
- Broecker, W. S., E. Clark, C. D. McCorkle, I. Hajdas, and G. Bonani (1999a), Core top ^{14}C ages as a function of latitude and water depth on the Ontong Java plateau, *Paleoceanography*, **14**, 13–22.
- Broecker, W. S., K. Matsumoto, E. Clark, I. Hajdas, and G. Bonani (1999b), Radiocarbon age differences between coexisting foraminiferal species, *Paleoceanography*, **14**, 431–436.
- Broecker, W. S., S. Barker, E. Clark, I. Hajdas, G. Bonani, and L. Stott (2004), Ventilation of the glacial deep Pacific Ocean, *Science*, **306**, 1169–1172.
- Broecker, W. S., S. Barker, E. Clark, I. Hajdas, and G. Bonani (2006), Anomalous radiocarbon ages for foraminifera shells, *Paleoceanography*, **21**, PA2008, doi:10.1029/2005PA001212.
- Emerson, S., and M. Bender (1981), Carbon fluxes at the sediment-water interface of the deep sea: Calcium carbonate preservation, *J. Mar. Res.*, **39**, 139–162.
- Higgins, S. M., W. Broecker, R. Anderson, D. C. McCorkle, and D. Timothy (1999), Enhanced sedimentation along the equator in the western Pacific, *Geophys. Res. Lett.*, **26**, 3489–3492.
- Keigwin, L. D. (2004), Radiocarbon and stable isotope constraints on Last Glacial Maximum and Younger Dryas ventilation in the western North Atlantic, *Paleoceanography*, **19**, PA4012, doi:10.1029/2004PA001029.
- Keir, R. S. (1984), Recent increase in Pacific CaCO_3 dissolution: A mechanism for generating old ^{14}C ages, *Mar. Geol.*, **59**, 227–250.
- Le, J. N., and R. C. Thunell (1996), Modelling planktic foraminiferal assemblage changes and application to sea surface temperature estimation in the western equatorial Pacific Ocean, *Mar. Micropaleontol.*, **28**, 211–229.
- Manighetti, B., I. N. McCave, M. Maslin, and N. J. Shackleton (1995), Chronology for climate change: Developing age models for the Biogeochemical Ocean Flux Study cores, *Paleoceanography*, **10**, 513–525.
- Murray, D. W. (1987), Spatial and temporal variations in sediment accumulation in the central tropical Pacific, Ph.D. thesis, Oregon State Univ., Corvallis.
- Oxburgh, R. (1998), The Holocene preservation history of equatorial Pacific sediments, *Paleoceanography*, **13**, 50–62.
- Peng, T. H., and W. S. Broecker (1984), The impacts of bioturbation on the age difference between benthic and planktonic foraminifera in deep-sea sediments, *Nucl. Instrum. Methods Phys. Res., Sect. B*, **233**, 346–352.
- Peng, T. H., W. S. Broecker, G. Kipphut, and N. J. Shackleton (1977), Benthic mixing in deep sea cores as determined by ^{14}C dating and its implications regarding climate stratigraphy and the fate of fossil fuel CO_2 , in *The Fate of Fossil Fuel CO_2 in the Oceans*, edited by N. R. Andersen and A. Malahoff, pp. 355–373, Springer, New York.
- Skinner, L. C., and N. J. Shackleton (2004), Rapid transient changes in northeast Atlantic deep water ventilation age across Termination I, *Paleoceanography*, **19**, PA2005, doi:10.1029/2003PA000983.
- Stuiver, M., P. J. Reimer, E. Bard, J. W. Beck, G. S. Burr, K. A. Hughen, B. Kromer, G. McCormac, J. Van der Plicht, and M. Spurk (1998), INTCAL98 radiocarbon age calibration, 24,000–0 cal BP, *Radiocarbon*, **40**, 1041–1083.
- Waelbroeck, C., J. C. Duplessy, E. Michel, L. Labeyrie, D. Paillard, and J. Duprat (2001), The timing of the last deglaciation in North Atlantic climate records, *Nature*, **412**, 724–727.

S. Barker, School of Earth, Ocean and Planetary Sciences, Cardiff University, Main Building, Park Place, Cardiff, CF10 3YE, UK.

W. Broecker and E. Clark, Lamont-Doherty Earth Observatory of Columbia University, 61 Route 9W, P.O. Box 1000, Palisades, NY 10964, USA.

I. Hajdas, AMS ^{14}C Laboratory, IPP ETH Hoenggerberg, CH-8093 Zurich, Switzerland.